Appl. Sci. Converg. Technol. 25(1): 19-24 (2016)
http://dx.doi.org/10.5757/ASCT.2016.25.1.19

Research Paper

Electronic Structure of Ce-doped ZrO_2 Film: Study of DFT Calculation and Photoelectron Spectroscopy

Kwang Sik Jeong[a], Jinho Song[a], Donghyuck Lim[a], Hyungsub Kim[b], and Mann-Ho Cho[a]*
[a]*Institute of Physics and Applied Physics, Yonsei University, Seoul 120-749, Korea*
[b]*School of Materials Science and Engineering, Sungkyunkwan University, Suwon*

Received December 31, 2015; revised January 13, 2016; accepted January 19, 2016

Abstract In this study, we evaluated the change of electronic structure during redox process in cerium-doped ZrO_2 grown by sol gel method. By sol-gel method, we could obtain cerium-doped ZrO_2 in high oxygen partial pressure and low temperature. After post annealing process in nitrogen ambient, the film is deoxidized. We used spectroscopic and theoretical methods to analysis change of electronic structure. X-ray absorption spectroscopy (XAS) for O K1-edge and Density Functional Theory (DFT) calculation using VASP code were performed to verify the electronic structure of the film. Also, high resolution x-ray photoelectron spectroscopy (HRXPS) for Ce 3d was carried out to confirm chemical bond of cerium doped ZrO_2. Through the investigation of the electronic structure, we verified as followings. (1) During reduction process, binding energy of oxygen is increase. Simultaneously, oxidation state of cerium was change to 4+ to 3+. (2) Cerium 4+ and cerium 3+ states were generated at different energy level. (3) Absorption states in O K edge were mainly originated by Ce 4+ f_0 and Ce 3+, while occupied states in valance band were mainly originated from Ce 4+ f_2.

Keywords: Electronic structure, Ce-doped ZrO_2, DFT Calculation, XPS, XAS

I. Introduction

Cerium doped ZrO_2 that generally called CSZ (cerium stabilized zirconium oxide), is used for several purposes related reduction process, such as oxygen reservoir and ionic conductor [1,2]. The chemical properties of cerium which has two oxidation states 3+ and 4+, makes it possible that large amount of reduction process [3]. When oxygen partial pressure is high, cerium are fully oxidized and become 4+ states. On the other hands, when oxygen partial pressure is low, cerium is deoxidized and become 3+ states. Therefore, cerium-doped ZrO_2 can store oxygen by change of partial pressure of oxygen or conduction of oxygen ion. Since application area of cerium-doped ZrO_2 is closely related with its chemical state, chemical property of cerium-doped ZrO_2 is intensively researched in many paper [4-6]. These researches are focus on chemical states of cerium with oxygen composition change or oxygen stores capacity. On the other hands, researches of electronic structure of cerium-doped ZrO_2 are relatively deficient, in spite of its interesting properties such as cerium f-orbital and various oxidation states. Therefore, in this study, we evaluated the electronic structure of cerium-doped ZrO_2 by combined spectroscopic and theoretical methods. Also, high resolution x-ray photoelectron spectroscopy (HRXPS) was carried out to confirm chemical bond of cerium-doped ZrO_2. Highly oxidized sample was prepared by sol-gel method in low temperature (300°C) and atmosphere pressure. Then post annealing at 700°C in nitrogen ambient was performed to deoxidize sample. We choose doping level of cerium 10% because significant change in crystal structure of ZrO_2 is not introduced. Therefore, effect of cerium reduction can be separated from the change in crystal structure. At the same time, 10% of cerium is enough portions to observe the modulation in electronic structure without structural change using spectroscopy method.

We observed two gap states at below conduction band edge in XAS spectrum. These intensities are modulated with change in oxidant state of cerium. Calculated electronic structure by DFT is support the experimental result which shows change in electronic structure during reduction process.

II. Experiment

We deposited 5-nm-thick ZrO_2 and cerium-doped ZrO_2 films using sol-gel synthesis [7]. Zirconium-n-butoxide was used as a base solution for ZrO_2 and cerium-doped ZrO_2. To incorporate cerium into the ZrO_2 film, approximately 10 mol % cerium nitrate hexahydrate was added to the base solution. Acetic acid and nitric acid were

*Corresponding author
E-mail: mh.cho@yonsei.ac.kr

used as the chelating agent and catalyst, respectively. Cerium nitrate hexahydrate was added to zirconium-n-butoxide, and the mixture was stirred for 3 hours to obtain a completely mixed solution. The sol was placed on the silicon substrate using a spin coater, and subsequently heated to 100°C. Finally, the sample was heated to 300°C in air to finalize the film synthesis. To modulate oxidation states of samples by redox, both films were annealed at 700°C under ambient nitrogen for 2 minutes.

XAS was performed to confirm the electronic structures of the ZrO_2 and cerium-doped ZrO_2 films using the synchrotron 8A1 beam line in Korea. The absorption spectra of O K_1-edge at photon energies ranging from 520 to 560 eV was measured using the total electron yield mode in the normal direction. Since metal oxides hybridize with oxygen 2*p* and 2*s*-orbitals, the O K_1-edge spectrum represents the electronic structure of the hybridized orbital. [8]. XAS spectrums are deconvoluted by Gaussian peaks The number of peaks was determined via crystal field theory.

HRXPS was performed using a monochromatic Al Ká X-ray source (1486.6 eV) to verify the chemical bonding of cerium-doped ZrO_2. Spectra were obtained for the chemical bonding states, including oxygen 1*s*, zirconium 3*d* and cerium 3*d*. All spectra were corrected to eliminate the charging effect using the carbon 1s peak at 285.0 eV. The background was removed using a Shirley-type subtraction, and the full-width at half maximum (FWHM) values of the constituent peaks were kept constant. Fitting curves were determined using Gaussian and Lorentzian distributions, in which the Gaussian distribution ratio was higher than 80%.

To verify origin of gap states that generated by Ce doping in ZrO_2, we performed DFT calculation. In our calculation, we used VASP code [9] with GGA PBESol [10] functional. We geometry optimized the monoclinic and tetragonal ZrO_2 structure with under 0.25/Ang k-spacing. Although the crystal structure of the as-grown films is amorphous, the atomic structure of the as-grown films was considered to be monoclinic. Considering that the amorphous structure in the DFT calculation requires a large unit cell that consumes computational time, the monoclinic and tetragonal ZrO_2 unit cell structure was geometrically optimized for both lattice parameter and atomic position, with a 6×6×6 k-point set and a 500-eV cut-off energy. For both unit cells, the initial structure followed those observed in the experimental results. Structure is relaxed until 0.02 eV/ang condition is satisfied. After geometry optimize, we build 2×2×2 supercell for monoclinic structure and 3×3×2 supercell for tetragonal to prevent mirror charge effect. Then we change one Zirconium to Cerium. Monoclinic structure system contains 31 Zirconium 1 Cerium and 64 oxygen. Tetragonal structure system contains 35 Zirconium 1 Cerium and 72 oxygen. For supercell calculation we choose 3×3×3 k-points. From XPS results, we made Ce 3+ by eliminate oxygen near doped Ce. Also, to simulate f_0, f_1 and f_2 states of Ce, we introduced 0, 1, 2 electrons in systems. Therefore, we present density of states for Ce 4+ f_0, f_1 and f_2 in monoclinic and tetragonal structure. In addition, density of states by Ce 3+ with 3-fold oxygen vacancy and 4-fold oxygen for monoclinic structure and Ce 3+ with oxygen vacancy for tetragonal structure are presented.

III. Result and Discussion

1. High resolution x-ray photoelectron spectroscopy (HRXPS)

Figure 1 represents zirconium 3d at a) and oxygen 1s at b) spectrum of XPS. In both as grown and annealed ZrO_2, a very clear and sharp zirconium 3d spectrum without any shoulder and broadness is obtained. The binding energy of peak is 182.3 eV, which is well consistent with reported values for zirconium oxide [11]. The spectrum can be deconvoluted by only one sub-peak that spin orbit splitting is 2.4 eV. The bonding characteristic of cerium doped ZrO_2 is is nearly same with the pure ZrO_2, as shown in the zirconium 3d spectrum. On the other hands, binding properties of oxygen in pure ZrO_2 are significantly different from that of the cerium doped ZrO_2, as shown at oxygen 1s spectra. The oxygen 1s spectrum for as-grown ZrO_2 can be deconvoluted with four sub-peaks, which are associated with oxygen interstitial (528.8 eV) ZrO_2 (530 eV), carbon oxide (531.6 eV) and silicon oxide (532.4 eV). In sol-gel method, ZrO_2 is synthetized in air under the high oxygen partial pressure. Accordingly, the ZrO_2 grown by sol-gel method can contain much interstitial oxygen [12]. In the as grown ZrO_2, the excess oxygen is contributed to the weak bonding. Therefore, it can be interpreted that highly oxidized film is successfully achieved by sol-gel method. After post-annealing process at nitrogen ambient, the excess oxygen in ZrO_2 diffused out as O_2 gas or reacted with silicon substrate. The removal of excess oxygen can be confirmed by decrease of low binding energy peak of oxygen 1s spectrum. Reaction with silicon substrate can be also verified by increase of silicon oxide peak in oxygen 1s spectra, comparing the as-grown ZrO_2 and annealed ZrO_2. Another important characteristic of ZrO_2 film grown by sol-gel method is that the peak with very high intensity caused by carbon oxide located at 531.6 eV is observed in both ZrO_2 and cerium-doped ZrO_2. Although the peak located at 531.6 eV, shown at oxygen 1s spectra, can be caused by ZrO_{2-X} or carbon oxide, it is more reasonable that the peak is resulted from the formation of carbon oxide because any ZrO_{2-X} peaks are not observed in zirconium 3d spectrum. Large amount of carbon oxide is reasonable because the samples are synthesized using carbon based solution process by sol-gel method.

Ce doped ZrO_2 shows different behavior: i.e., there is no oxygen interstitial peak in both as-grown and annealed Ce doped ZrO_2. Doping of lanthanides to ZrO_2 stabilize

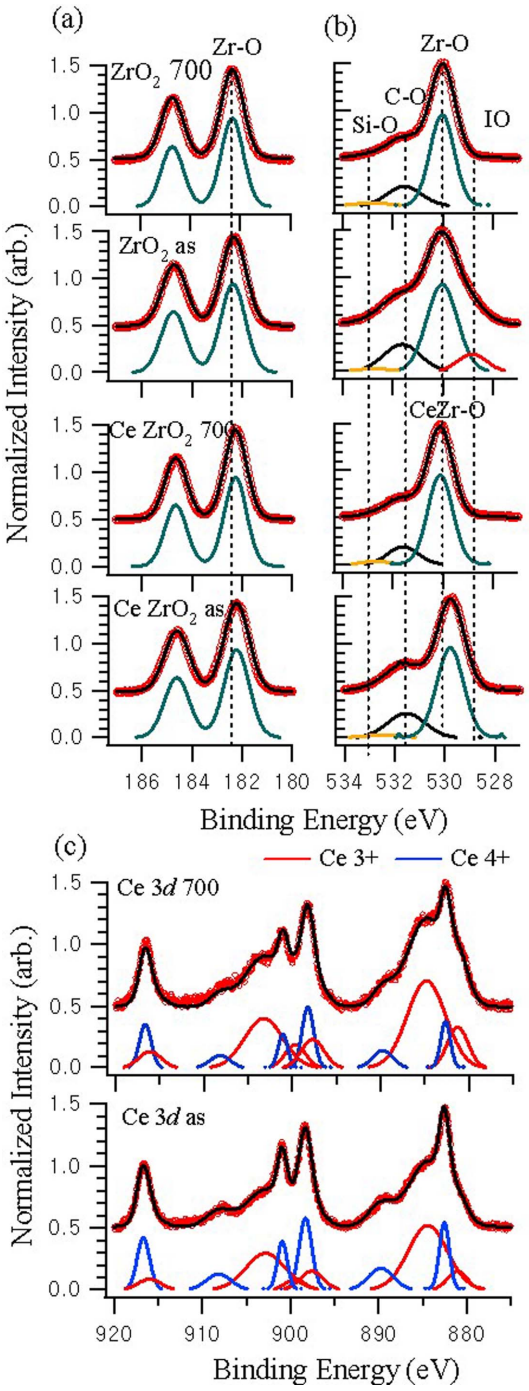

Figure 1. XPS spectra for (a) Zr 3d spectra for annealed un-doped ZrO_2, as-grown un-doped ZrO_2, annealed Ce-doped ZrO_2 and as-grown Ce-doped ZrO_2 (b) O 1s spectra for annealed un-doped ZrO_2, as-grown un-doped ZrO_2, annealed Ce-doped ZrO_2 and as-grown Ce-doped ZrO_2 (c) Ce 3d spectra for Ce-doped ZrO_2 for annealed Ce-doped ZrO_2 and as-grown Ce-doped ZrO_2.

oxygen deficiency [13]. Therefore, doping of Ce increase formation energy for oxygen intestinal, which well explains the change in chemical state. After annealing process, binding energy of CeZr-O is shift to lower energy. This shift is larger than that of ZrO_2. By Ce doping, change amount oxygen proportion become larger. This is possible due to transition of Ce oxidation states which is shown in Fig 1(c) Ce 3d spectra.

Red colored peaks in Fig 1(c) are correlated to the chemical bonding states of cerium 3+. Blue colored peaks are associated with cerium 4+. Each bonding is deconvoluted with three peaks, which are originated from many body charge transfer effects of f-orbitals of cerium. Since f-orbital of cerium has two empty states at lower energy than its Fermi level, when core hole generated, electron is transferred to empty states and lower Fermi level in order to screen effect of core hole. Therefore cerium has three states in f-orbital as shown in XPS spectra which are non(f_0), one(f_1) and two(f_2) electron-occupied states. The shape of blue colored peaks in the XPS spectra is consistent to previously reported bond of cerium 4+: i.e., f0, f_1 and f_2 peaks arise at 883.8 eV, 890.8 eV and 899.7 eV. The peak differences in Δf_0-f_1 and Δf_1-f_2 are 7.0 eV and 8.9 eV, respectively. The value of the spin-orbit splitting and its relative intensity is 18.4 eV and 0.73. In addition, red colored peaks are in accord with reported cerium spectra of cerium 3+: i.e., f_0, f_1 and f_2 peaks are observed at 882.2 eV, 886.1 eV and 898.6 eV, where Δf_0-f_1 is 3.9 eV and Δf_1-f_2 is 12.5 eV. The value of the spin-orbit splitting and relative intensity is 18.4 eV and 0.57. The relative intensity and the energy separation of the peaks are in good agreement with the reported result [14,15]. As shown in Fig 1(c), composition of Ce3+ and Ce4+ is dramatically changed after annealing process. When Ce doped ZrO_2 is highly oxidized, composition of Ce4+ is similar to composition of Ce3+. When film is deoxidized by annealing process, intensity of Ce4+ peaks is decreased while intensity of peaks is increased.

2. X-ray absorption spectroscopy (XAS)

Oxygen K-edge XAS spectra of as-grown and annealed ZrO_2 are shown in lower side of Fig. 2. XAS spectra represent the energy state in conduction band caused by the arrangement of oxygen around transition metal of metal oxide film. The first states denoted by e_g are lowest energy state in the conduction band owing to two-fold degeneration, which is associated with d_{x2-y2} and d_{z2} component of oxygen position. The next states of t_{2g} are resulted from tri fold degeneration, which is related with d_{xy}, d_{yz} and d_{zx}. The trifold degeneration also generates the third states of t1g state, which is constituted by three degenerated states of p_x, p_y, and p_z. The last states of a1g are caused by s-orbital of transition metal, not degenerated states. In as-grown ZrO_2 spectrum in Fig. 2, the energy difference between two peaks of t_{2g} and e_g, about 3.2 eV, is caused by Crystal field splitting. The first peak of e_g can be deconvoluted into two peaks with the energy difference of 1.20 eV. The second peak of t_g can be also deconvoluted into three peaks which are separated by 1.3 eV and 1.4 eV. The increase in the energy difference between t_{2g} and e_g after the annealing treatment at 700°C can be closely related to Crystal field effect: i.e., the increase in the energy

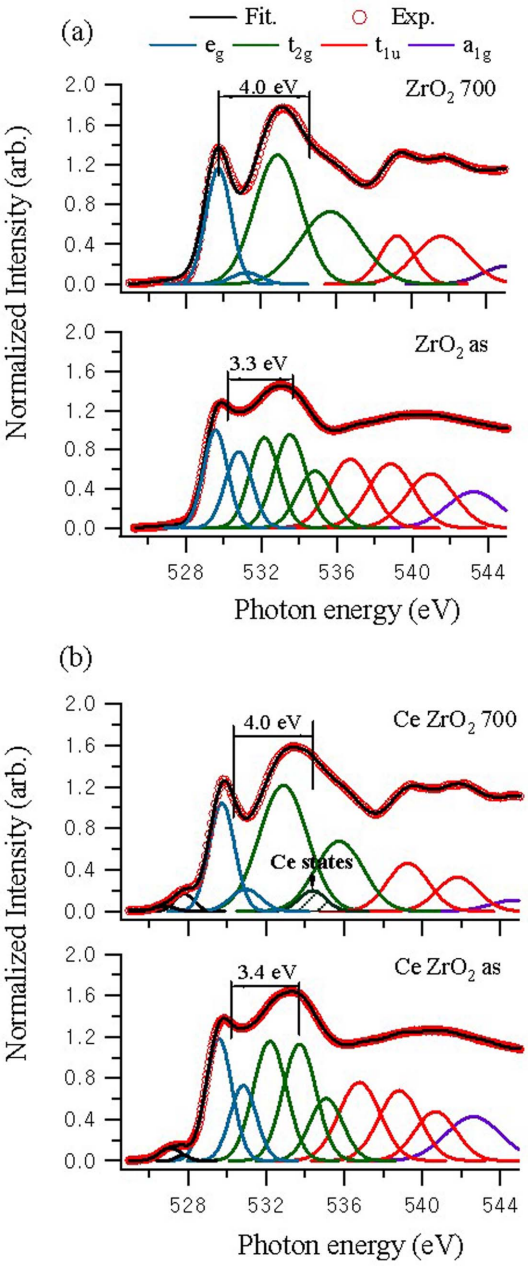

Figure 2. XAS spectra for (a) annealed un-doped ZrO2 and as-grown un-doped ZrO_2 (b) annealed Ce-doped ZrO_2 and annealed Ce-doped ZrO_2.

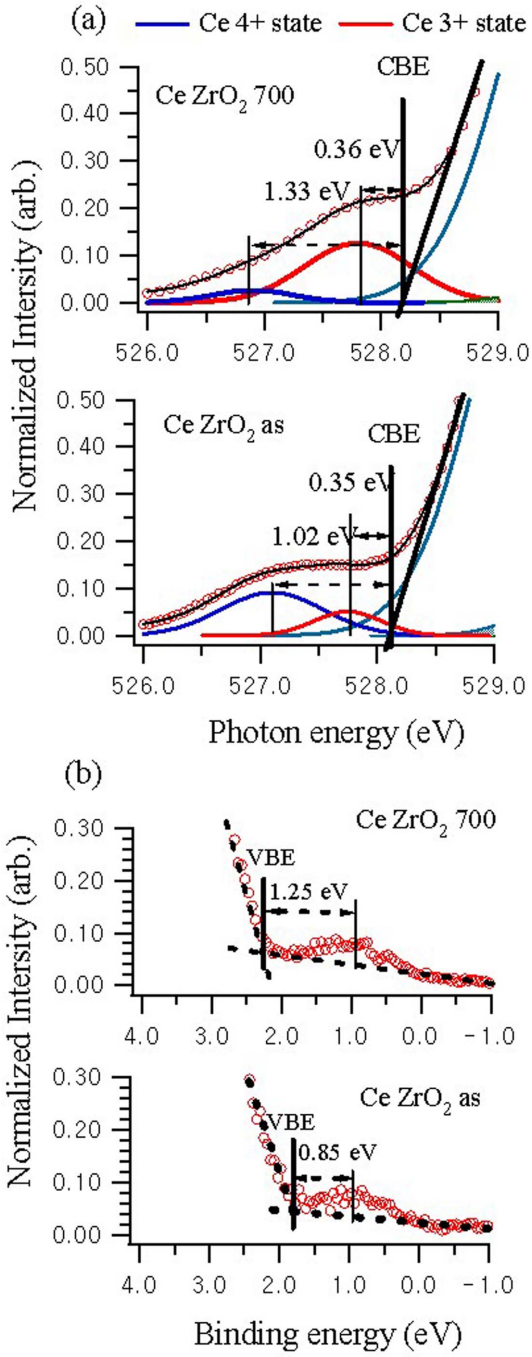

Figure 3. (a) Pre-edge magnification of XAS spectra for annealed Ce-doped ZrO_2 and as-grown Ce-doped ZrO_2 (b) XPS Valance band spectra for Ce-doped ZrO_2 and as-grown Ce-doped ZrO_2

difference is enhanced as the crystal structure is changed to cubic-like structure. The peak splitting in t_{2g} and t_{1g} is caused by Jhan-Teller effect: i.e., since the degenerated states are changed from monoclinic to tetragonal structure, the 3 peak splitting in t_{2g} and t_{1g} is changed to 2 peak splitting. Thus degeneration of d_{zx} and d_{yz} is still remaining in tetragonal structure, resulting in deconvoluted two energy states with the energy difference of 2.9 eV. Similarly, t1u state that consists with p_x, p_y and p_z, can be deconvoluted into two peaks in tetragonal structure. Therefore, broken degenerations induce the change in the energy states: i.e., the 3 degenerated states are changed to 2 states, separated by d_{x2-y2} and d_{z2} for e_{1g}, d_{xy}, d_{yz}, and d_{zx} for t_{2g}, p_x, p_y, p_z for t1g in tetragonal structure. Moreover, the increase in the energy difference between e_g and t_{2g} caused by Crystal field splitting can be clearly illustrated because the tetragonal structure is more cubical structure than monoclinic structure [16].

XAS spectra in 528 eV to 544 eV range for Ce doped ZrO_2 is similar to spectra of ZrO_2. Peak position of each states almost same within 0.1 eV. This means similarity in crystal structure of ZrO_2 and Ce doped ZrO_2. Considering that As-grown Ce doped ZrO_2 is monoclinic and annealed

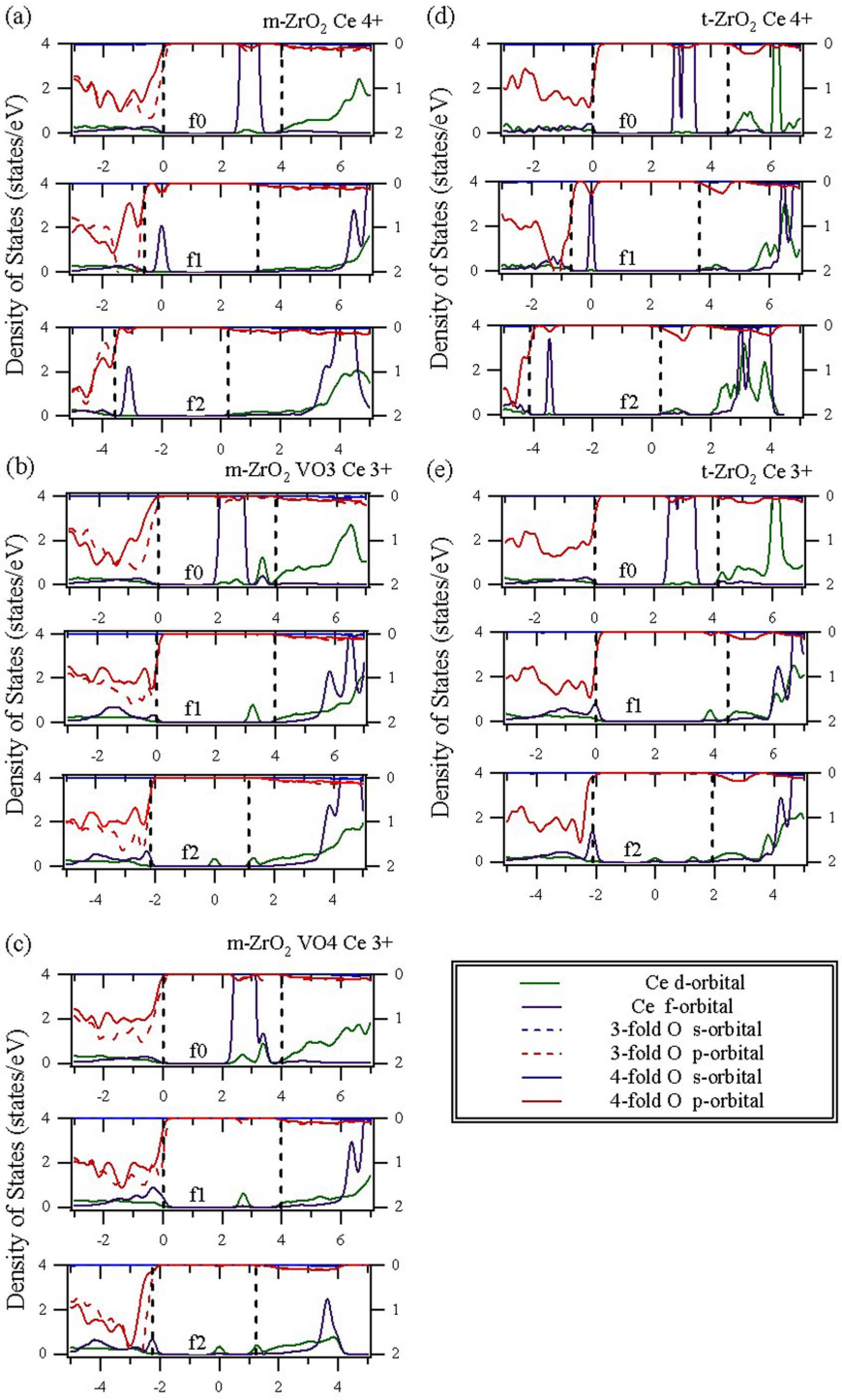

Figure 4. Density of states for Ce and bonded oxygen (a) Ce 4+ of monoclinic Ce-ZrO_2 (b) Ce 3+ with 3-fold oxygen vacancy of monoclinic Ce-ZrO_2 (c) Ce 3+ with 4-fold oxygen vacancy of monoclinic Ce-ZrO_2 (d) Ce 4+ of tetragonal Ce-ZrO_2 (e) Ce 3+ with oxygen vacancy of tetragonal Ce-ZrO_2.

ZrO_2 is tetragonal, small difference in spectra for this range is originated from Ce-O hybridized state. Since amount of this states is ~ 1/10, comparing with Zr-O hybridization states, it is hard to deconvolute the peak in as-grown film. When film is annealed only, one Ce states is deconvoluted in t_{2g} states. On the other hands, pre-edge absorption of Ce doped ZrO_2 is totally different from pre-edge absorption of ZrO_2. Although there is no observable pre-edge absorption both as-grown and annealed ZrO2, large pre-edge absorption for Ce doped ZrO_2 is oobserved. In Fig 3(a), XAS pre-edge absorption states for Ce-doped ZrO_2 are presented. By Ce doping, two states is generated at 0.35 eV and 1.02 eV from conduction band edge (CBE). Absorption intensity of states which is located at 1.02 eV from CBE is larger than that of states located at 0.36 eV from CBE. When film is annealed, position and relative intensity of absorption is changed:. i.e., peak positions of the two states are shifted to 1.33 eV and 0.36 eV from

CBE. Relative absorption intensity of closer from CBE become larger. XPS Ce 3d spectra result which shows change in oxidation states Ce 4+ to Ce 3+ imply that two pre-edge states is originated from different oxidized Ce. For annealed tetragonal structure, Ce 3+ is generated closer from CBE state and Ce 4+ is generated far from CBE state. For monoclinic structure, by DFT calculation result, we conclude that absorption peak located at 1.03 eV from CBE is caused by Ce 3+ with four-fold oxygen vacancy and Ce 4+. While absorption peak at 0.35 eV from CBE is originated from Ce 3+ with three-fold oxygen vacancy. In order to measure the occupied chemical state of the ZrO_2 film, XPS valance band spectra was obtained, as shown in Fig 3(b). In as-grown Ce-doped ZrO_2 film, there is one peak exist at 0.85 eV from valance band edge (VBE). When sample is annealed, this peak shift to 1.25 eV from VBE. Not like unoccupied states in XAS spectra, gap state cannot be deconvoluted to two peaks. With DFT calculation, we verified that occupied state contains only Ce 4+ originated state.

3. DFT Calculation

In monoclinic structure, Ce 4+ generates unoccupied states at 1.0 eV from CBE when Ce 4+ is f_0 state. Ce 4+ also generate occupied state at 0.3 eV from VBE when Ce 4+ is f_2 state. These states shift by crystal structure change to tetragonal. Unoccupied Ce 4+ f_0 state is located at 1.2 eV from CBE. Occupied Ce 4+ f_2 state is located at 0.3 eV from 0.5 eV. In monoclinic structure, two kind oxygen exist; ie 3-fold oxygen and 4-fold oxygen. Absence of 3-fold or 4-fold oxygen gNenerate different gap-state. Ce 3+ f_1 with 3-fold oxygen vacancy generates some states at 0.5 eV from CBE. Ce 3+ f_1 with 4-fold oxygen vacancy generate a state at 1eV from CBE which is overwrapped with Ce 4+ f_0 state. Therefore, Ce 3+ state with 4-fold oxygen vacancy can't be deconvoluted from Ce4+ f_0 state in experiment. In tetragonal structure there is only one kind oxygen state: i.e., Ce 3+ f_1 with oxygen vacancy generates a state at 0.5 eV from CBE.

This result is consistent with the observed XAS and XPS result. By annealing process, crystal structure is changed from monoclinic to tetragonal. At the same time, state located at far from CBE is shifted 1.02 eV to 1.33 eV. State which is located at 0.35 eV from CBE is not shift. Gap state in XPS valance band spectrum is also shift from 0.85 eV to 1.25 eV with the transformation of crystal structure. Although, exact states position are different by DFT error for transition metal, the peak change in experimental data ca be well descried by calculation result.

IV. Conclusions

In this study, we observed the change in electronic structure of Ce doped ZrO_2 with oxygen content change by annealing in nitrogen ambient. As-grown Ce doped ZrO_2 which is synthesized by sol-gel method in 300ºC air, is monoclinic structure. After annealing process crystal structure changed to tetragonal. In XPS spectra, chemical shift of oxygen 1s ZrCe-O bond is occurred by deoxidation after the annealing process. At the same time, in Ce 3d spectra, transformation of Ce 4+ to Ce3+ by deoxidation is observed. By Ce doping, gap states are generated, which is confirmed by XAS pre-edge absorption and XPS valance band spectra. Performing DFT calculation, we concluded that these states are originated from Ce 4+ f_0, f_2 and Ce 3+ f_1. Ce f_2 generates occupied states, which is consistent with XPS valance spectra.

References

[1] Kašpar J, Fornasiero P, and Graziani M. Use of CeO2-based oxides in the three-way catalysis. Catal Today. 50(2) 285-98 (1999).
[2] Hasegawa Y, Imanaka N, and Adachi G-y. Cerium ion conducting solid electrolyte. J Solid State Chem. 171(1-2) 387-90.
[3] Skorodumova NV, Simak SI, and Lundqvist BI, Abrikosov IA, Johansson B. Quantum Origin of the Oxygen Storage Capability of Ceria. Phys Rev Lett. 89(16) 166601 (2002).
[4] Suda A, Sobukawa H, Suzuki T, Kandori T, Ukyo Y, and Sugiura M. Store and Release of Oxygen of Ceria-Zirconia Solid Solution Synthesized by Solid Phase Reaction at Near Room Temperature. J Ceram Soc Jpn. 109(1267) 177-80 (2001).
[5] Sugiura M. Oxygen Storage Materials for Automotive Catalysts: Ceria-Zirconia Solid Solutions. Catal Surv Asia. 7(1) 77-87 (2003).
[6] Mamontov E, Egami T, Brezny R, Koranne M, and Tyagi S. Lattice Defects and Oxygen Storage Capacity of Nanocrystalline Ceria and Ceria-Zirconia. The Journal of Physical Chemistry B. 104(47) 11110-6 (2000).
[7] Lee MS, An C-H, Park K, Choi J-Y, and Kim H. Effect of Y, Gd, Dy, and Ce Doping on the Microstructural and Electrical Properties of Sol-Gel-Deposited ZrO_2 Film. J Electrochem Soc. 158(6) G133-G6 (2011).
[8] De Groot F and Kotani A. Core level spectroscopy of solids: CRC press; 2008.
[9] Kresse G and Hafner J. Ab initio molecular dynamics for open-shell transition metals. Phys Rev B Condens Matter. 48(17) 13115-8 (1993).
[10] Perdew JP, Burke K, and Ernzerhof M. Generalized Gradient Approximation Made Simple. Phys Rev Lett. 77(18) 3865-8 (1996).
[11] Gutowski M, Jaffe JE, Liu C-L, Stoker M, Hegde RI, Rai RS, et al. Thermodynamic Stability of High-K Dielectric Metal Oxides ZrO_2 and HfO2 in Contact with Si and SiO2. MRS Online Proceedings Library. 716 null-null (2002).
[12] Jeong KS, Song J, Lim D, Lee MS, Kim H, and Cho M-H. Structural evolution and defect control of yttrium-doped ZrO_2 films grown by a sol-gel method. Appl Surf Sci. 320 128-37 (2014).
[13] Machida M, Kawano T, Eto M, Zhang D, and Ikeue K. Ln Dependence of the Large-Capacity Oxygen Storage/Release Property of Ln Oxysulfate/Oxysulfide Systems. Chem Mater. 19(4) 954-60 (2007).
[14] Bêche E, Charvin P, Perarnau D, Abanades S, and Flamant G. Ce 3d XPS investigation of cerium oxides and mixed cerium oxide (CexTiyOz). Surf Interface Anal. 40(3-4) 264-7 (2008).
[15] Romeo M, Bak K, El Fallah J, Le Normand F, and Hilaire L. XPS Study of the reduction of cerium dioxide. Surf Interface Anal. 20(6) 508-12 (1993).
[16] Burns RG. Mineralogical applications of crystal field theory: Cambridge University Press; 1993.